

Role of cofilin-1 during epithelial-mesenchymal transition in colorectal cancer cells

Annie C. M. Sousa-Squiavinato (DO), Renata Ivo Vasconcelos, Murilo Ramos Rocha, Pedro Barcellos-de-Souza, and Jose Andrez Morgado-Diaz
 Cell Structural and Dynamics Group, Cell and Molecular Oncobiology Program - Brazilian National Cancer Institute (INCA), Rio de Janeiro, Brazil
 Email: anniecrith@gmail.com; jmorgado@inca.gov.br

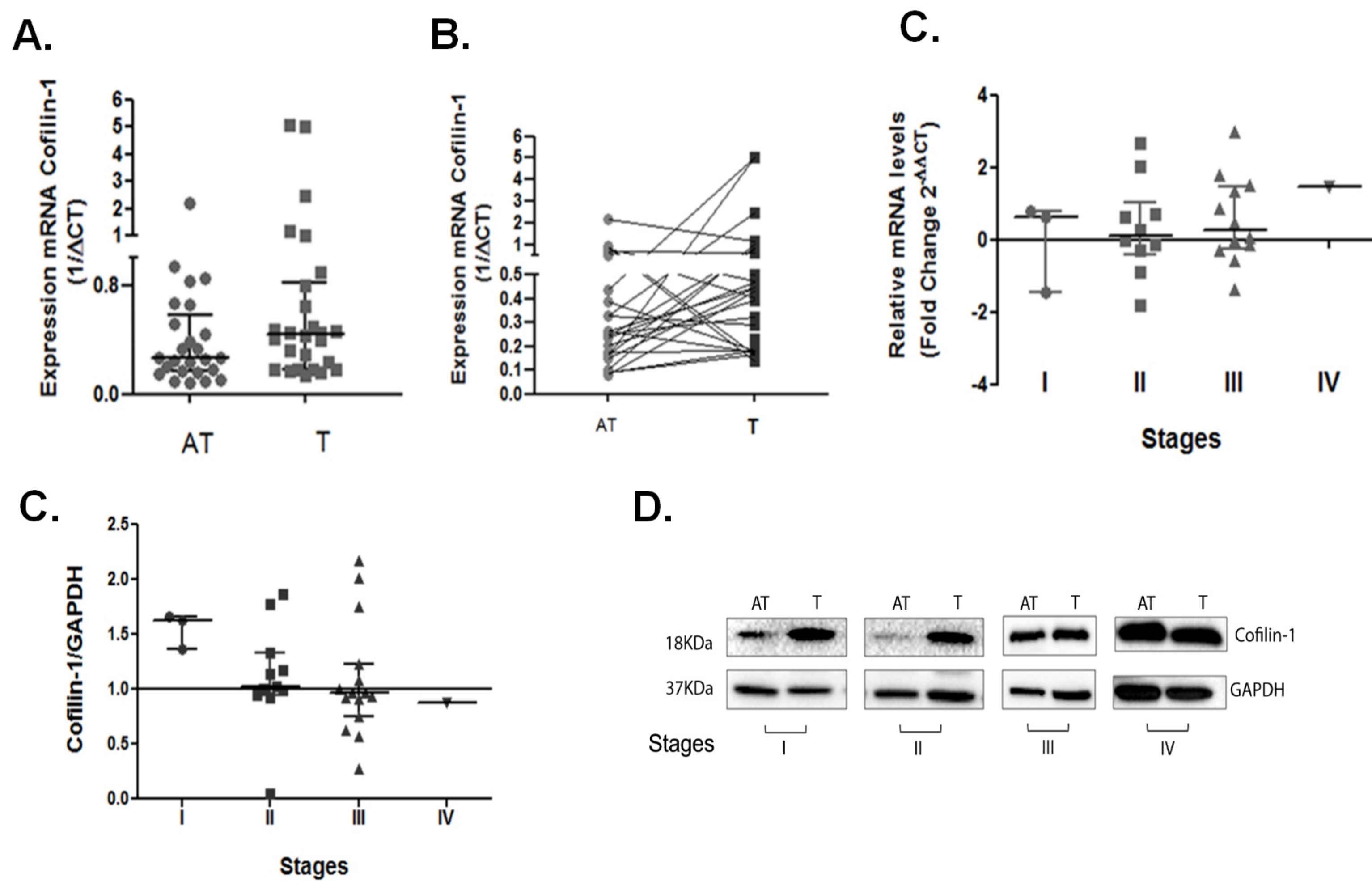


Figure 1-Expression genic of Cofilin in tumor samples from CRC. The levels of Cofilin in tumor tissues (T) were measured in relation to the levels of normal adjacent (AT) respective. (A) General information of the mRNA levels of Cofilin in tumor samples. (B) Evaluation of mRNA levels of cofilin-1 in adjacent tissue samples with paired samples of tumor tissue from the same patient. (C) Analysis of Cofilin mRNA levels in tumor samples separated by staging. n = 26. (D) Expression protein analysis of Cofilin in samples of adjacent tissue and tumor tissue in stages I, II and III (n = 33). Data representative of median and interquartile. (E) Representative images of protein levels of Cofilin in samples from patients with CRC.

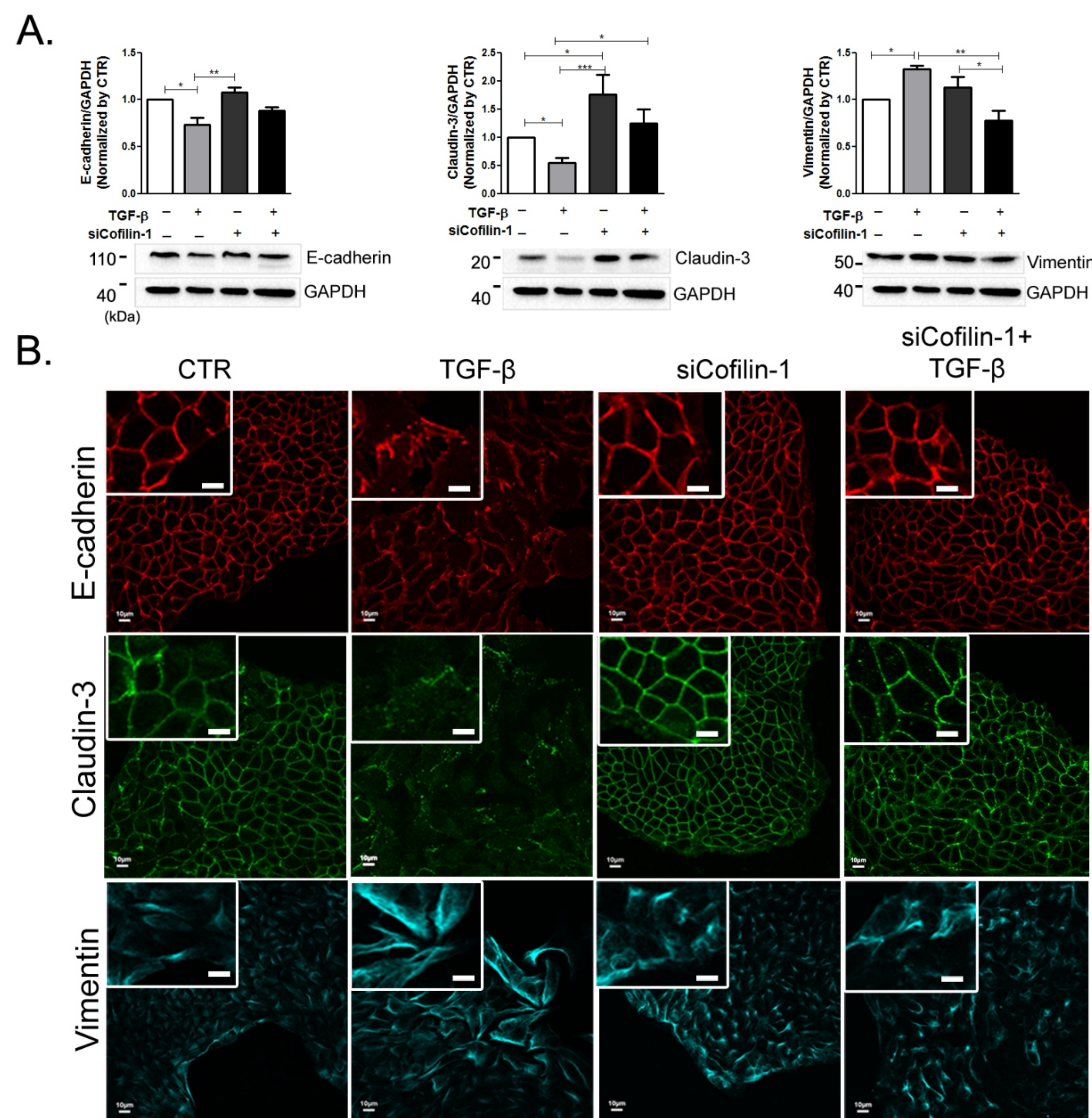


Figure 2- Effects of cofilin-1 silencing on switch between epithelial and mesenchymal states in TGF- β -treated cells. (A) HT-29 cells were transfected with si-CTR or siCofilin-1 and untreated or treated with TGF- β for 48 h. Western blotting and densitometric analysis of E-cadherin, claudin-3, and vimentin are shown. GAPDH was used as a loading control. (B) Representative immunofluorescence images of E-cadherin and claudin-3 obtained by confocal microscopy of HT-29 cells transfected with si-CTR or siCofilin-1 and treated with TGF- β for 48 h. Fluorescence images of Cy3-vimentin localization are also shown. Scale bar: 10 μ m

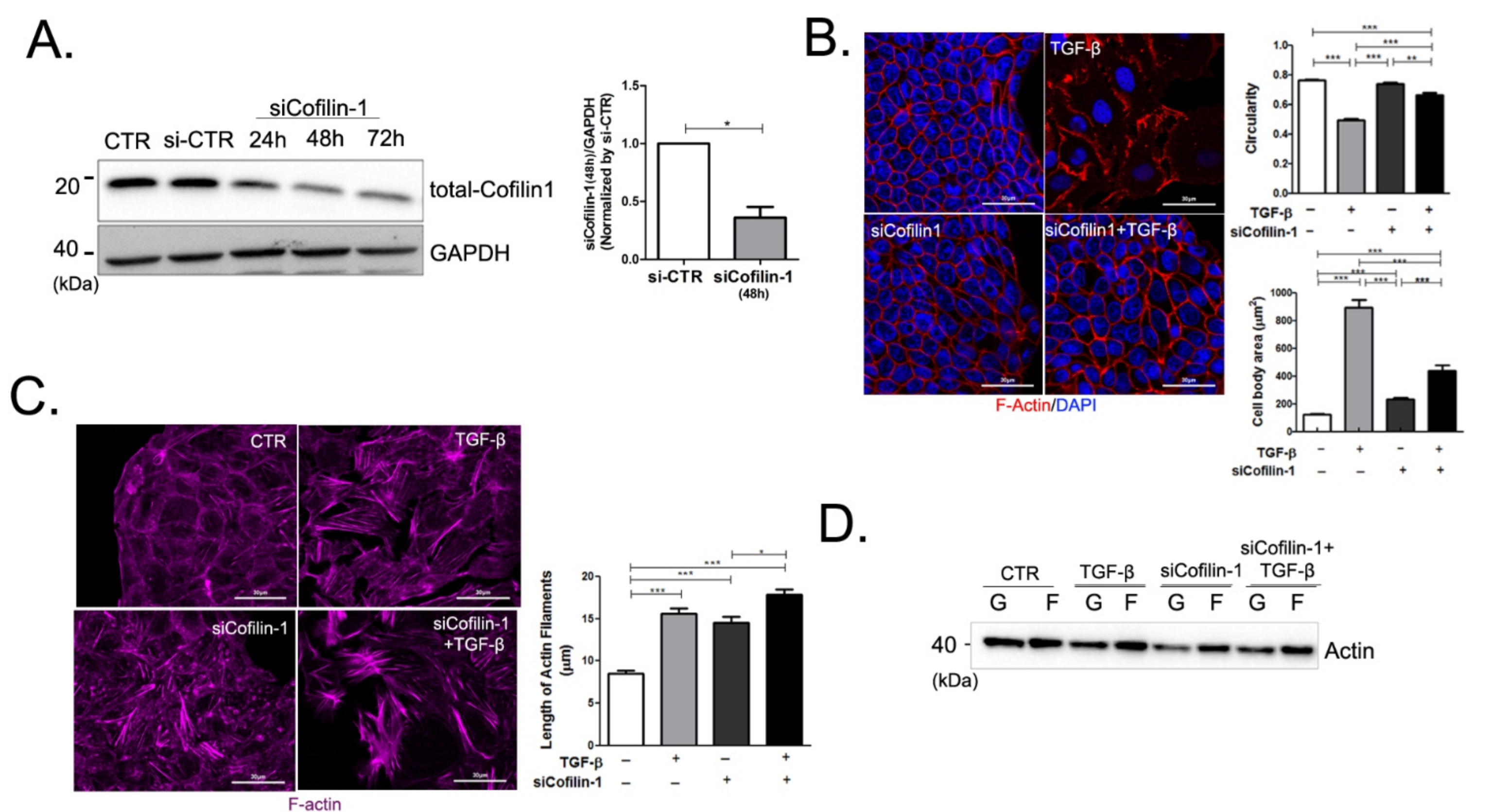


Figure 3- Effects of cofilin-1 silencing on cell morphology and actin cytoskeletal rearrangements in TGF- β -treated cells. (A) HT-29 cells were transfected with si-CTR or siCofilin-1 at the indicated times. (B) Cell circularity and cell body area were determined from immunofluorescence images in the middle Z-stack using ImageJ software. (C) Length of actin filament bundles was detected using maximum intensity projections by confocal microscopy and quantified using ImageJ software. (D) Quantification of G- and F-actin cellular fractions obtained by Triton X-100 fractionation. A representative western blot is shown. Scale bar in B and C: 30 μ m

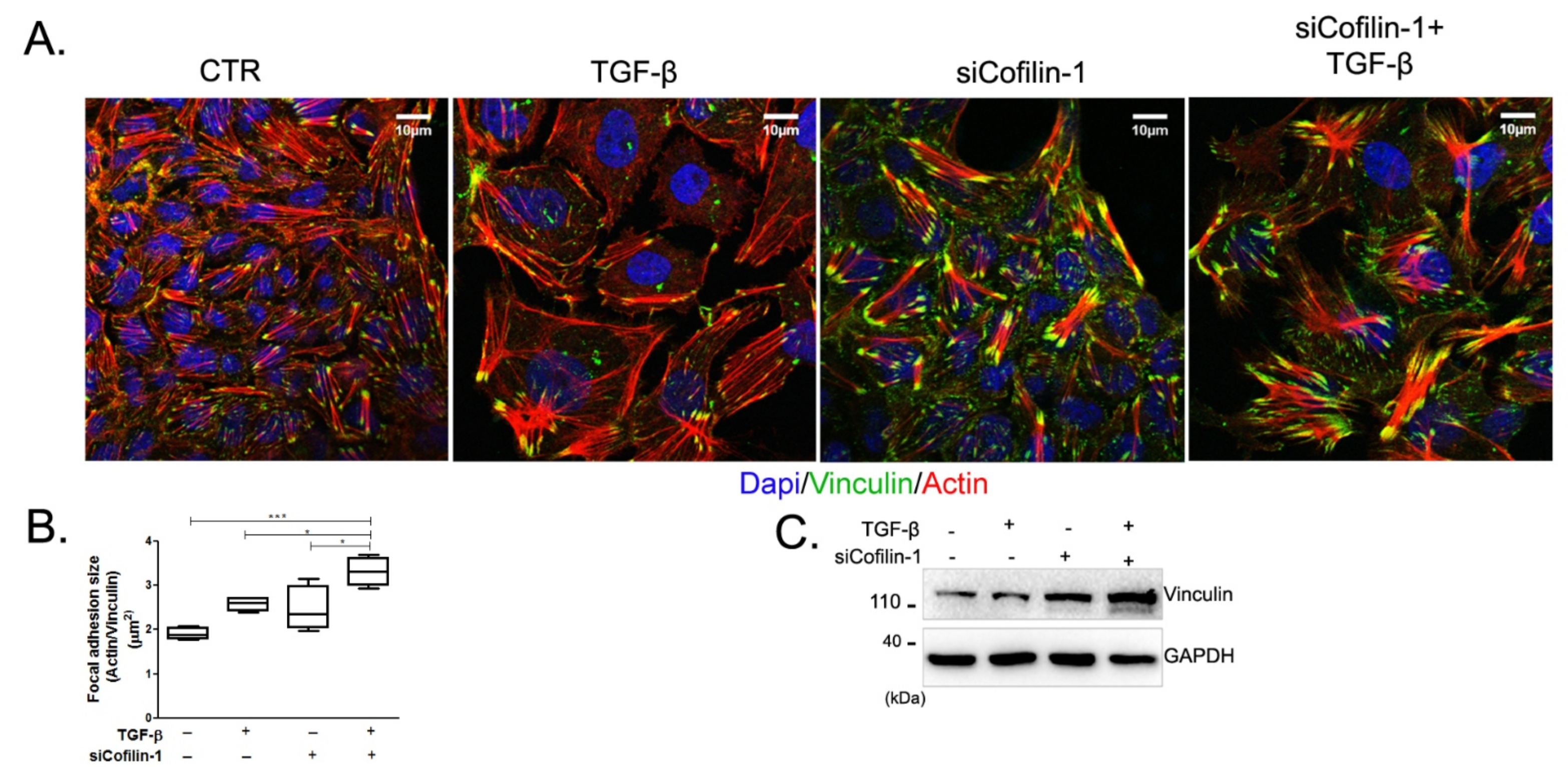


Figure 4- Role of cofilin-1 depletion in organizational pattern of focal adhesions. HT-29 cells were transfected with si-CTR or siCofilin-1 and untreated or treated with TGF- β (10 ng/mL) for 48 h. (A) Cells were grown on glass coverslips and subjected to immunofluorescence analysis of vinculin and actin localization. Scale bar: 10 μ m. (B) Focal adhesion size was calculated using ImageJ software through colocalization of vinculin and actin labeling. (C) HT-29 cells were lysed and analyzed by western blot analysis.

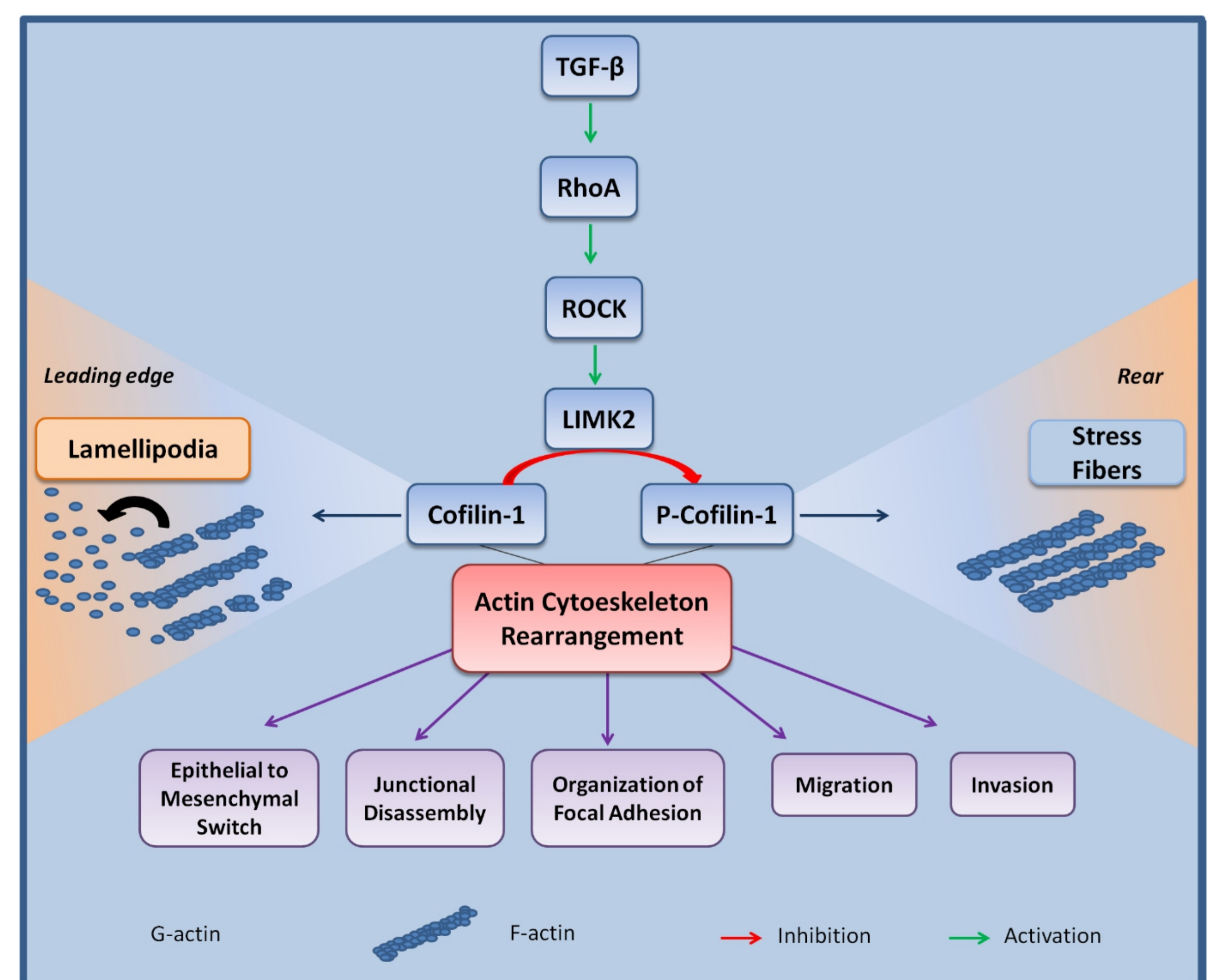


Figure 5- Schematic representation of the cofilin-1 pathway signaling in EMT cells. TGF- β activates RHOA signaling, leading to the activation of the Cofilin-1 regulation cycle, mediated by phosphorylation of LIMKs. So, this cycle occurs in different cell regions and regulates the organization of the actin cytoskeleton. At the front of the cell, active Cofilin-1 is concentrated, participating in the severing and polymerization of the nascent filaments in lamellipodium. At the rear of the cell, P-Cofilin-1 concentrates by regulating the formation of stress fibers, important for cell support and traction force. This cytoskeleton dynamic led deregulation of adhesion cell systems and increase of migration and invasion in EMT cells.